

Optimal Design of a Delayed Feedback

N. Semenic¹, A. Sarjas², A. Chowdhury¹, R. Svecko²

¹Margento R&D d.o.o.,

Gospodarska c. 84, 2000 Maribor, Slovenia

²Faculty of Electrical Engineering and Computer Science, University of Maribor,

Smetanova St. 17, 2000 Maribor, Slovenia

nikolaj.semenic@margento.com

Abstract—In this paper robustness analysis and simultaneous stabilization of a semiconductor laser (SL) with a delayed optoelectronic feedback (OEF) is studied. Using the theory of stability radius maximal allowed norm bounded perturbations of the SL in contrast to stabilizable intervals of OEF parameters are obtained. Using proposed algorithms we can analyse the effect of interdependencies of uncertainties of the OEF and SL parameters and design an optimal OEF according to specific robustness constraints.

Index Terms—Robust stability, delay systems, semiconductor lasers, laser feedback.

I. INTRODUCTION

Analysis of plants with time delays has attracted great interests in the last three decades [1]. Time delays are present in many applications and areas [2], ranging from biology, process control, logistics, telecommunications, to semiconductor lasers (SLs) [3], which are indispensable in many sensor applications [3], [4] or optical communications [5], [6].

Especially when a SL is used in a specific application, its operating features, which depend on its stability, robustness and dynamics characteristics are of huge importance. Many characteristics can be affected by the use of OEF which can be applied to any laser diode [3]. OEF is a connection from the optical laser output, which is detected by a photodetector to the injection current at the input. The detected photocurrent is amplified and fed back to the injected current as a positive or negative amount (Fig. 1). Typical result of such a feedback is shown in regular or irregular (chaotic) pulsations in the output. By appropriate setting of the feedback parameters stable and fast pulses with specific pulse width can be easily obtained [3]. In this way high coherent light source can be achieved. Many applications use such a light source as for example laser range finders, markers, designators, night vision goggles, rifle sights, LIDAR, 3D optical data storage [7]. In recent years the use of such systems has been attractive in secure chaos communications [6]. The use of OEF introduces a delay to the system as a consequence of time responses of a detector and electronic circuits. The design and implementation of OEF is therefore certainly not trivial as different physical disturbances acting on closed loop system might affect the

system to such an extent that stable output pulsation might become chaotic.

In this paper we are interested in the optimal design of the OEF in sense of robust stabilization and chaos suppression in the SL output [3], [8]. We have followed the steps from [9] as far as computation of robustness of specific parameters is concerned and applied an improved method in the sense of efficient computation. We obtained maximal bounds of SL parameters uncertainties in contrast to simultaneously stabilizable intervals of OEF parameters. We propose numerical algorithms for derivation of such intervals inside of uncertainties sets. According to proposed algorithms and applied specific criteria optimal OEF design parameters can be determined, which guarantee certain amount of bounded perturbations of the SL and its OEF parameters. All the proposed algorithms were implemented using MATLAB® and evaluated on a SL model [3]. Presented results can be adapted and used for any other system that contains time delays.

The mathematical model of the SL with OEF is described in Section II. Stability and robustness analysis is presented in Sections III and IV. Simultaneous stabilization and optimal OEF design is addressed in Section V. Design examples and conclusion are given in Sections VI and VII.

II. SEMICONDUCTOR LASER WITH OPTOELECTRONIC FEEDBACK

The dynamics of a SL with OEF (Fig. 1) can be described with two equations of the photon number and the carrier density. The mathematical model is represented with the following rate equations [3]:

$$\frac{dS(t)}{dt} = \left[G_n \{n(t) - n_{th}\} \right] S(t), \quad (1)$$

$$\frac{dn(t)}{dt} = \frac{J(t)}{ed} \left\{ 1 + \xi \left(\frac{S(t-\tau) - S_{off}}{S_s} \right) \right\} - \frac{n(t)}{\tau_s} - G_n \{n(t) - n_0\} S(t), \quad (2)$$

where S is the photon number, G_n is the gain coefficient, n is the carrier density, n_{th} is the carrier density at threshold, J is the injected current density, d is the thickness of the active layer, e is the elementary positive charge constant, ξ is the feedback strength, S_{off} is the constant offset in the feedback loop, S_s is the steady state value for the photon number, n_0 is

Manuscript received December 11, 2014; accepted September 3, 2014.

Operation has been partly financed by the European Union, European Social Fund.

the carrier density at transparency, τ_s is the lifetime of the carrier, and τ is the feedback time delay. See [10] for the details of those parameters.

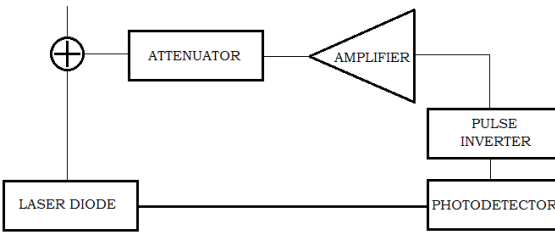


Fig. 1. Semiconductor laser with optoelectronic feedback.

Local dynamics of SL with OEF might be investigated using linear stability analysis. According to [3], [8] the linearization procedure applied to (1) and (2) results in the following characteristic equation in variable λ with one delay term $e^{-\frac{\lambda\tau}{a}}$

$$\lambda^2 + a(c^2 + 1)\lambda + c^2 \left(1 + \gamma e^{-\frac{\lambda\tau}{a}}\right), \quad (3)$$

which can be represented as a delay differential equation (DDE) [11]

$$\dot{x}(t) = \begin{bmatrix} 0 & 1 \\ -c^2 & -a(c^2 + 1) \end{bmatrix} x(t) + \begin{bmatrix} 0 & 0 \\ -\gamma c^2 & 0 \end{bmatrix} x\left(t - \frac{\tau}{a}\right), \quad (4)$$

where $a = v^{-0.5}$, v is the ratio of the photon damping rate in the cavity to the rate of population relaxation, $c = c_0/(\sqrt{1+\gamma})$, where $c_0 = \sqrt{q-1}$, where $q = (\tau_s J)/(edG_n n_s)$ is the pumping rate, n_s is steady state carrier density and $\gamma = \xi J/(edS_s)$ is the feedback coefficient. Values of the parameters [3] are listed in Table I.

TABLE I. PARAMETERS OF THE SL [3].

Symbol	Value	Description
v	10^3	the ratio of the photon damping rate in the cavity to the rate of population relaxation
q	1.5	pumping rate
$a = v^{-0.5}$	$3.1623 \cdot 10^{-2}$	parameter depending on the ratio v
γ	parameter	feedback gain
τ	parameter	feedback time delay
$c_0 = \sqrt{q-1}$	$7.0711 \cdot 10^{-1}$	frequency of relaxation oscillations
$c = \frac{c_0}{\sqrt{1+\gamma}}, \gamma \neq 1$	$5 \cdot 10^{-1}$	parameter depending on the pumping rate and the feedback gain

From the stability analysis of (3) boundary of stable and unstable oscillations of the laser can be determined (Fig. 2).

As was reported in [8] this curves correspond to the stable and unstable boundaries of the rate equations (1) and (2). As will be shown in our further analysis local stability boundaries might rapidly change by perturbations of certain parameters. Beyond these bounds the laser output is subjected to various irregular oscillations, which extend from regular pulsing over quasi-periodic pulsing to chaotic pulsing, where chaotic pulses have both chaotic peak intensities and chaotic pulse intervals.

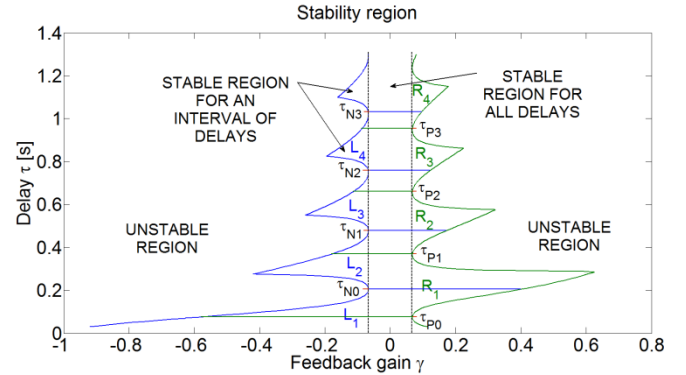


Fig. 2. Stability margins with R_x and L_x regions.

To assure stable output laser oscillations despite certain perturbations of parameters analysis of robustness must be taken into account.

III. STABILITY ANALYSIS

Stability of a time delay system can be determined by its eigenvalues, which should be located in the open left half plane [2], [12]. There are several methods that provide numerical algorithms for eigenvalues computation of a time delay system [13]–[18]. Stability boundaries concerning feedback gain in contrast to time delay were determined using an improved version of [14] according to the Algorithm I.

The [14] is based on the computation of all eigenvalues in the selected half plane via spectral discretization and on the estimation procedure of the desired discretization points. In addition, a correction method of derived eigenvalues is used. But there is a drawback, the region of the computation must be set manually. The larger is the selected region the more expensive and time consuming is the computation. On the other hand, the computation is unsuccessful if the region doesn't contain any eigenvalues. For determination of the stability region of (3) only the rightmost eigenvalue is needed. We have improved the algorithm [14] in a manner to derive only few rightmost eigenvalues by means of automatic selection of computation region. In this way an efficient algorithm for determination of stability boundaries of (3) has been constructed in MATLAB®.

Algorithm I. Computation of few rightmost eigenvalues:

1. Initialize computation region $\{R(\lambda) \geq r | \lambda \in \mathbb{C}\}$, $r = -\tau/3$ and execute estimation procedure of discretization points N of [14]. If $N_{min} = 10 < N < N_{max} = 100$ is met go to step 4.
2. If $N > N_{max}$ iteratively decrease region $r = r + 5$ and save $r_1 = r$ until $N_{min} < N < N_{max}$ or if $N < N_{max}$ save $r_2 = r$. If $N < N_{min}$ iteratively increase region $r = r - 5$ and save $r_1 = r$ until $N_{min} < N < N_{max}$ or if $N > N_{max}$ save $r_2 = r$. If $N_{min} < N < N_{max}$ is met go to step 4.
3. Iteratively select $r = (r_1 + r_2)/2$ using bisection algorithm until $N_{min} < N < N_{max}$ is met.
4. Calculate eigenvalues using spectral discretization method [14].

Using the Algorithm I stability margins for negative γ_N and positive γ_P gain values of (3) were determined for the following set of time delays (Fig. 2 and Fig. 3)

$$\tau_i = \{0.03 + i0.005 | i \in \mathbb{N}^0 \wedge 0 \leq i \leq 254\}. \quad (5)$$

IV. ROBUSTNESS ANALYSIS

Perturbations of certain parameters might rapidly change stability bounds and influence regular SL output oscillation to such an extent that it might become chaotic. In what follows, maximal allowed perturbations (h) [9] were computed for stable region of OEF parameters $(\tau_i, \gamma_{i,j})$ using proposed implementation.

A. Stability Radius

Maximal allowed perturbations of a time delay system, which shift its eigenvalues to imaginary axes, can be determined using complex stability radius, which is defined by [9]

$$r_C = \left(\sup \mu_\Delta \left(\mathbf{M}(j\omega) \left(j\omega I - \mathbf{A}_0 - \sum_{i=1}^m \mathbf{A}_i e^{-j\omega\tau_i} \right)^{-1} \mathbf{N}(j\omega) \right) \right)^{-1}, \quad (6)$$

where μ_Δ is a structured singular value and can be computed using the *mussv* routine in MATLAB®, matrices \mathbf{M} and \mathbf{N} define certain structure of perturbations, $\lambda I - \mathbf{A}_0 - \sum_{i=1}^m \mathbf{A}_i e^{-\lambda\tau_i}$ for $\lambda = j\omega$ is a characteristic equation of a time delay system with system matrices $\mathbf{A}_0, \dots, \mathbf{A}_m$. Applying additive perturbations to (4), where $h = \max\{|h_0|, |h_1|, |h_2|, |h_3|\} < r_C$ holds

$$\begin{aligned} \dot{x}(t) = & \begin{bmatrix} 0 & \frac{1}{a} \pm \delta h_0 \\ -\frac{c^2}{a} \pm \delta h_1 & -(c^2 + 1) \pm \delta h_2 \end{bmatrix} x(t) + \\ & + \begin{bmatrix} 0 & 0 \\ -\gamma \frac{c^2}{a} \pm \delta h_3 & 0 \end{bmatrix} x(t-\tau), \end{aligned} \quad (7)$$

where $\delta \in [0, 1]$, results in following matrices:

$$\left\{ \begin{array}{l} \mathbf{M}(j\omega) = \begin{bmatrix} 0 & 1 \\ 1 & 0 \\ 0 & 1 \\ e^{-j\omega\tau_k} & 0 \end{bmatrix}, \\ \mathbf{N}(j\omega) = \begin{bmatrix} 1 & 0 & 0 & 0 \\ 0 & 1 & 1 & 1 \end{bmatrix}. \end{array} \right. \quad (8)$$

B. Efficient Computation of Stability Radii for the Semiconductor Laser

Computation of numerous stability radii on a 2-D grid (Fig. 3) of stable region is a demanding task due to the complex nature of structured singular value problem, which in addition needs to be evaluated over an interval of ω (6). The computation was performed over the set (5) and following stable sets of feedback gains

$$\begin{aligned} \gamma_{i,j}(\tau) = & \{\gamma_{N_i}(\tau_i) + j0.01 | j \in \mathbb{N}^0 \wedge 0 \leq \\ & \leq j < \gamma_{P_i}(\tau_i) / 0.01\} \cup \{\gamma_{P_i}(\tau_i)\}. \end{aligned} \quad (9)$$

To reduce the complexity of computation we propose Algorithm II.

Algorithm II. Computation of stability radius:

1. For each $\tau_i, \gamma_{i,j}$ compute magnitude $M_1 = \| (j\omega I - \mathbf{A}_0 - \sum_{i=0}^m \mathbf{A}_i e^{-j\omega\tau_i})^{-1} \|_2$ on an interval of $\omega_1 = [0, 10\pi/\tau_i]$ with step size $s_1 = 0.01\pi/\tau_i$.
2. Extract two thirds of the largest M_1 with corresponding ω_1 as M_2 and ω_2 .
3. Compute stability radius r_1 (6) over the ω_2 with step size of s_1 .
4. When the algorithm stops, rectangle with the largest τ_Δ is selected and saved, as well as τ_c and γ_c .

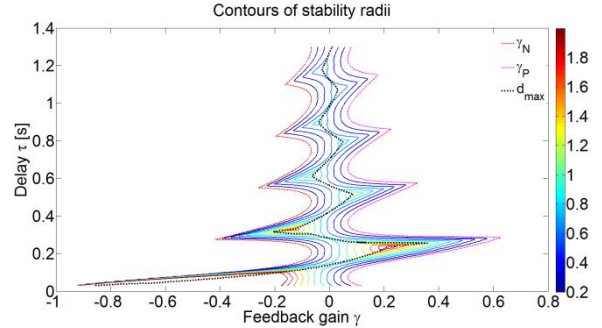


Fig. 3. Contours of stability radii plotted for $\epsilon_n = \{0.2, 0.4, \dots, 1.8, 2.0\}$.

Step size was constructed as a function of time delay to assure appropriate precision also for higher values of time delays. With higher delays eigenvalues condense towards the origin of the complex plane [2], which results also in condensed picks in magnitude. For that reason smaller step size is needed.

Figure 3 shows results of the stability radii for the stable region (Fig. 2). The highest levels of stability radii are displaced from the center of the stable region. With increased values of the stability radii stability margins start to narrow until individual connected contours are derived.

V. SIMULTANEOUS STABILIZATION

Another important aspect of robustness concerns the time delay. As a result of different external influences the time delay in the OEF might change and cause instability. Figure 3 clearly denotes the reduction of the areas surrounded by individual contours when the amounts of perturbations increase. The higher are perturbations of parameters the more limited become stability bounds and the admissible intervals of gains and delays decrease.

A. Simultaneous Stabilization

Computation of maximal stabilizable intervals $(\tau_\Delta, \gamma_\Delta)$ of feedback parameters (τ, γ) in contrast to maximal allowed parameters perturbations ($h(\tau, \gamma)$) was carried out for all contours of stability radii inside of regions of R_1 and L_2 (Fig. 2). Individual regions are defined as:

$$R_x := \gamma_N \cap \gamma_P \cap \tau \geq \tau_{P_{x-1}} \cap \tau \leq \tau_{P_x}, \quad (10)$$

where $x = 1, 2, 3, 4$.

$$L_x := \begin{cases} \gamma_N \cap \gamma_P \cap \tau > 0 \cap \tau \leq \tau_{N_0}; x = 1, \\ \gamma_N \cap \gamma_P \cap \tau \geq \tau_{N_{x-2}} \cap \tau \leq \tau_{N_{x-1}}; x = 2, 3, 4. \end{cases} \quad (11)$$

The goal was to obtain the largest possible rectangular

shape inside of each contour (Fig. 3 and Fig. 4). By choosing the centred points (τ_c, γ_c) of such rectangles optimal feedback parameters $(\tau_{opt}, \gamma_{opt})$ can be obtained which allow bounded parameters perturbations (h) and simultaneous stabilization on delay (τ_Δ) and gain intervals (γ_Δ) of certain desired size.

To obtain $\tau_{c,n,k}$, $\gamma_{c,n,k}$ and corresponding $\tau_{\Delta,n,k}$ for each contour ϵ_n and for $\gamma_{\Delta,n,k}$ we propose Algorithm III.

Algorithm III. Computation of $\tau_{c,k}$, $\gamma_{c,k}$ and $\tau_{\Delta,k}$ intervals for $\gamma_{\Delta,k} = \{k0.005|k = 1, 2, \dots\}$:

1. Each contour $\epsilon_n = \{n0.005|n = 1, 2, \dots\}$ of $h_{i,j}$ was extracted, up sampled to delay and gain step size of 0.0001 and divided into upper and lower set of points.
2. For each point A the corresponding C , D and B points were found (Fig. 4). C was found using a bisection algorithm.
3. The formation of rectangles proceeds until points occur inside of the rectangle. Only first time rectangles are calculated for all upper points. Next iterations use the information of the position of previously selected maximal rectangle in Step 4.
4. When the algorithm stops, rectangle with the largest τ_Δ is selected and saved, as well as τ_c and γ_c .

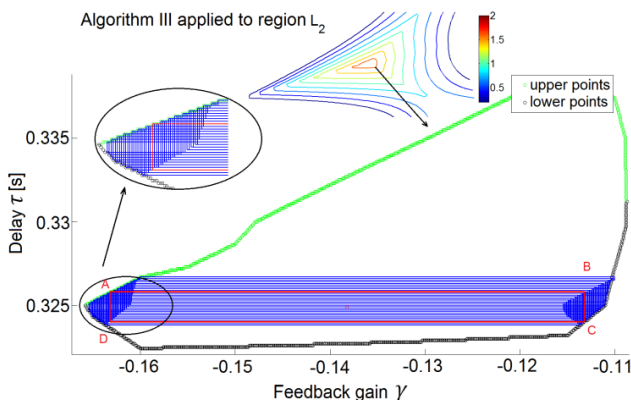


Fig. 4. Algorithm III: Out of blue rectangles the red rectangle is chosen with maximal interval of delays.

Figure 5 and Fig. 6 show results of the Algorithm III evaluated over contours in region R_1 . Figure 5 represents inverse dependence of τ_Δ and ϵ_n to γ_Δ .

Figure 6 represents τ_c , γ_c for which τ_Δ and γ_Δ at specific ϵ_n can be achieved. For higher values of ϵ_n smaller stabilizing intervals can be achieved, which clearly shows that it is impossible to obtain maximal robustness of the SL and OEF.

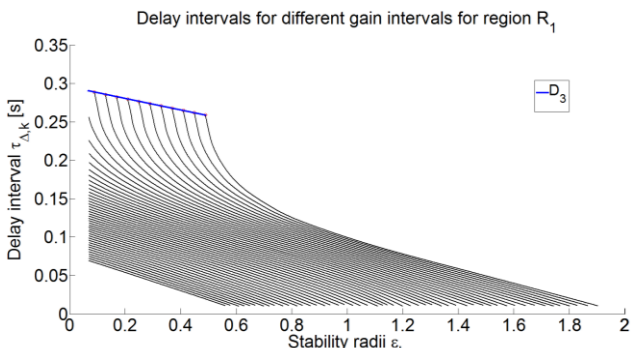


Fig. 5. Each curve represents $\tau_{\Delta,k}$ obtained for specific ϵ_k belonging to R_1 for $\gamma_{\Delta,k} = \{0.01, 0.02, \dots, 0.49, 0.50\}$ (right to left).

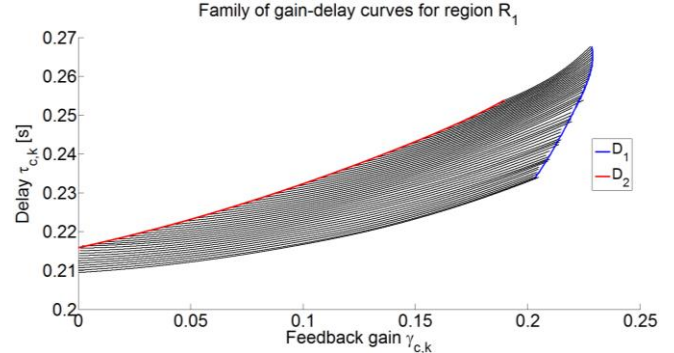


Fig. 6. $\tau_{c,k}$, $\gamma_{c,k}$ values for R_1 depicted for $\gamma_{\Delta,k} = \{0.01, 0.02, \dots, 0.49, 0.50\}$ (down-up).

B. Interpolation of Families of Curves

Resulting curves of (τ_c, γ_c) and $(\tau_\Delta, \epsilon_n)$ can be represented by several groups of polynomials, which can be derived using curve fitting tool *cftools* in MATLAB®.

Family of curves of (τ_c, γ_c) , belonging to region R_1 (Fig. 6), bounded by the area $T_c \in D_1 \cap D_2 \cap \tau_c > 0 \cap \gamma_c \geq 0$, where D_1 and D_2 are derived using fourth order polynomial fitting, is described as a group of polynomials

$$T_c(\gamma_\Delta, \gamma_c) = a_3(\gamma_\Delta) \gamma_c^3 + a_2(\gamma_\Delta) \gamma_c^2 + a_1(\gamma_\Delta) \gamma_c + a_0(\gamma_\Delta), \quad (12)$$

with polynomial coefficients defined as

$$a_i(\gamma_\Delta) = b_{i,3}\gamma_\Delta^3 + b_{i,2}\gamma_\Delta^2 + b_{i,1}\gamma_\Delta + b_{i,0}, \quad (13)$$

where $i = 3, 2, 1, 0$. $T_\Delta(\gamma_\Delta, \epsilon)$ belonging to R_1 , bounded by $T_\Delta \in D_3 \cap \epsilon > 0.07 \cap \tau_\Delta > 0.01$, where D_3 is derived using linear line fitting, is described using polynomials

$$T_\Delta(\gamma_\Delta, \epsilon) = a_3(\gamma_\Delta) \tau_\Delta^3 + a_2(\gamma_\Delta) \tau_\Delta^2 + a_1(\gamma_\Delta) \tau_\Delta + a_0(\gamma_\Delta) \tau_\Delta. \quad (14)$$

In order to achieve accurate fitting we can divide the whole family of curves into several groups of polynomials (12) or (14). Polynomials (12) and (14) were derived using proposed Algorithm IV.

Algorithm IV. Interpolation of a family of curves:

1. Family of curves is divided into several groups according to γ_Δ , ϵ or γ_Δ , γ_c .
2. For each group interpolate all curves and save coefficients.
3. Interpolate evolution of individual coefficients of polynomials to derive (13) and describe the whole group with (12) or (14) respectively.

C. Correction Algorithm

Obtained polynomials $T_c(\gamma_\Delta, \gamma_c)$ were used to correct corresponding polynomials $T_\Delta(\gamma_\Delta, \epsilon)$ with the help of the Algorithm I and proposed Algorithm V. Correction of each polynomial was executed for 15 distinct points.

Algorithm V. Correction of $T_\Delta(\gamma_\Delta, \epsilon)$:

1. Reduce $T_\Delta(\gamma_\Delta, \epsilon)$ by 0.02 and keep evaluating Algorithm I for (7) using data of $T_c(\gamma_\Delta, \gamma_c)$ increasing $T_\Delta(\gamma_\Delta, \epsilon)$ by 0.02 till stability is compromised.

2. Use bisection algorithm to determine corrected maximal $\tilde{\tau}_\Delta$ with tolerance of 0.0001.

The maximal stable delay interval τ_Δ was computed for all four extreme points in a rectangle. For values of uncertainties ϵ_n all possible combinations of signs of individual perturbations had to be taken into account, as maximal allowed perturbation is provided as absolute value. Obtained corrected curves $(\tilde{\tau}_\Delta, \epsilon)$ were expressed in terms of polynomials \tilde{T}_Δ using (14) and Algorithm IV.

D. Optimal Optoelectronic Feedback Design

Using simple search routine along derived groups of polynomials it is possible to obtain τ_{opt} and γ_{opt} settings of the OEF which meet the criteria of simultaneous stabilization on desired intervals τ_Δ and γ_Δ at specific maximal allowed perturbations ϵ of the SL parameters.

VI. OPTIMAL OPTOELECTRONIC FEEDBACK DESIGN EXAMPLE

We consider SL with OEF with uncertain time delay $\tau = 0.28 \pm 0.05$ s, gain uncertainty $\gamma_\Delta \geq 0.05$ and uncertain parameters $\epsilon \geq 0.2$. Let's find the optimal OEF gain γ_{opt} in the sense of maximal possible parameters uncertainty ϵ .

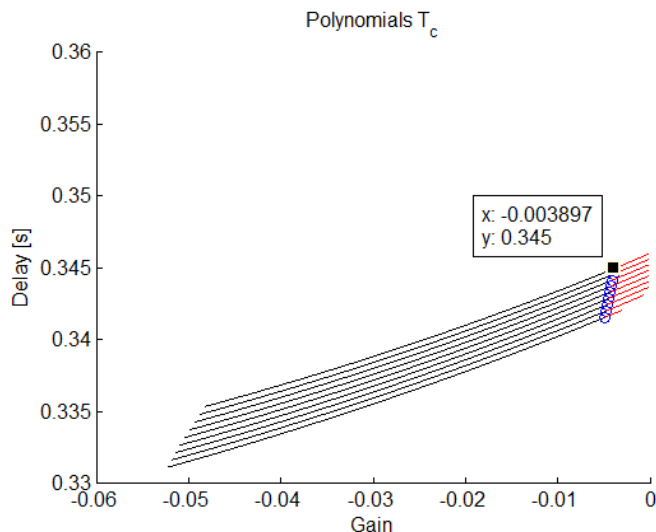


Fig. 7. Group of polynomials belonging to L_2 fulfilling the required criteria.

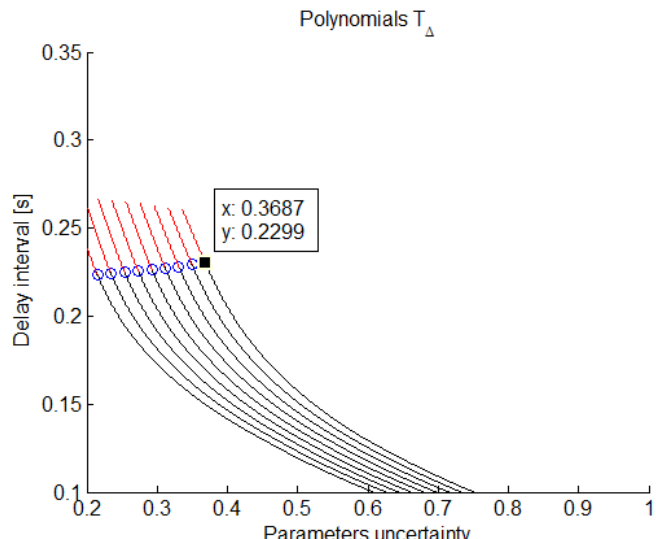


Fig. 8. Group of polynomials belonging to L_2 fulfilling the required criteria.

Polynomials $\tilde{T}_\Delta(\gamma_\Delta, \epsilon)$ and $T_c(\gamma_\Delta, \gamma_c)$ which meet required criteria in region L_2 are shown in Fig. 7 and Fig. 8 in red. Maximal possible $\epsilon = 0.3687$ is obtained for $\gamma_\Delta = 0.05$ and $\tau_\Delta = 0.23$ s (Fig. 8) at $\gamma_{opt} = -0.0039$ and $\tau_{opt} = 0.345$ s ($\tau_1 = \tau_{opt} - \tau_\Delta/2 = 0.23$ s, $\tau_2 = \tau_{opt} + \tau_\Delta/2 = 0.46$ s, $\tau \in [\tau_1, \tau_2]$), (Fig. 7).

Considering region R_1 and the above criteria, $\tilde{T}_\Delta(\gamma_\Delta, \epsilon)$ and $T_c(\gamma_\Delta, \gamma_c)$ are obtained as depicted in Fig. 9 and Fig. 10 in red. Maximal possible $\epsilon = 0.3691$ is obtained for $\gamma_\Delta = 0.05$ and $\tau_\Delta = 0.236$ s (Fig. 10) at $\gamma_{opt} = 0.0075$ and $\tau_{opt} = 0.215$ s ($\tau_1 = \tau_{opt} - \tau_\Delta/2 = 0.1$ s, $\tau_2 = \tau_{opt} + \tau_\Delta/2 = 0.33$ s, $\tau \in [\tau_1, \tau_2]$), (Fig. 9).

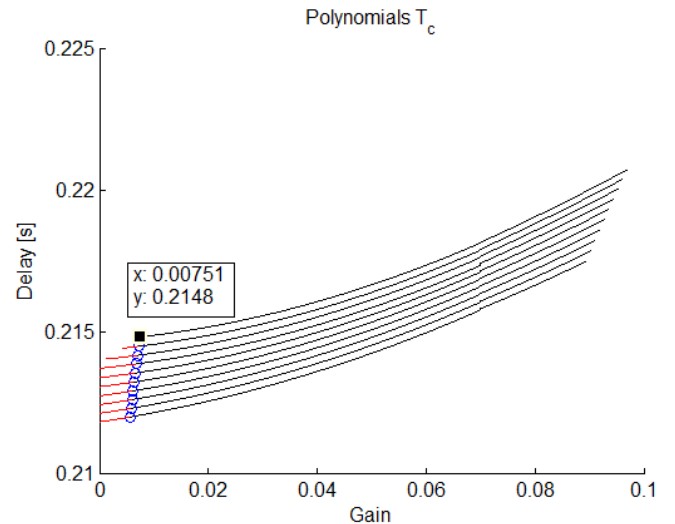


Fig. 9. Group of polynomials belonging to R_1 fulfilling the required criteria.

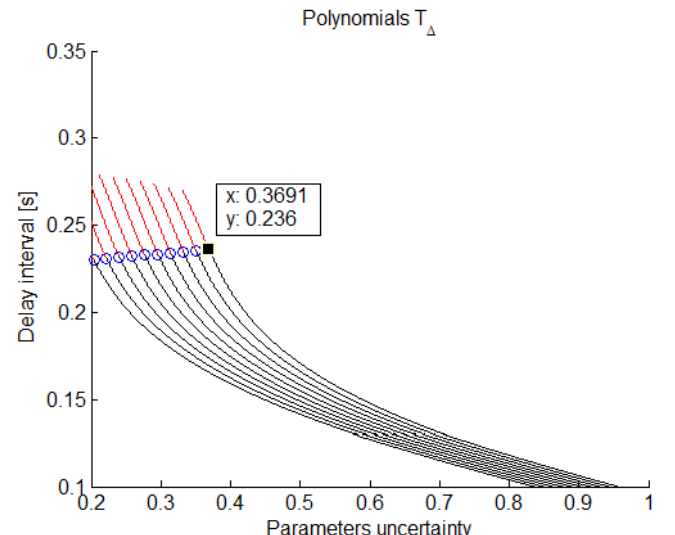


Fig. 10. Group of polynomials belonging to R_1 fulfilling the required criteria.

In this example we have presented two possible solutions in terms of the required criteria. The optimal gain setting fulfilling all the requirements was achieved for maximal uncertainty of $\epsilon = 0.3691$ at feedback gain value of $\gamma_{opt} = 0.0075$.

VII. CONCLUSIONS

In the presented work stability and robustness of the SL were studied with special concern devoted to the simultaneous stabilization on the intervals of the OEF

parameters in contrast to uncertainties of the SL parameters, which was evaluated using several algorithms. Improved numerical algorithms for computation of stability radius and stability boundaries in terms of computation of only few rightmost eigenvalues were provided.

As was shown, amounts of simultaneously stabilizable OEF intervals inversely depend on the values of SL parameters perturbations, which imply that it is impossible to obtain maximal robustness of the SL and the OEF parameters. In this manner an optimal OEF might be designed considering specific constraints and criteria as discussed in provided example.

Proposed algorithms can be adapted and used for any other time delay system.

REFERENCES

- [1] J.-P. Richard, "Time-delay systems: an overview of some recent advances and open problems", *Automatica*, vol. 39, no. 10, pp. 1667–1694, 2003. [Online]. Available: [http://dx.doi.org/10.1016/S0005-1098\(03\)00167-5](http://dx.doi.org/10.1016/S0005-1098(03)00167-5)
- [2] W. Michiels, S. Niculescu, *Stability and Stabilization of Time-Delay Systems. An Eigenvalue Based Approach*, Philadelphia: SIAM Publications, 2007, ch. 1. [Online]. Available: <http://dx.doi.org/10.1137/1.9780898718645>
- [3] Junji Ohtsubo, *Semiconductor Lasers, Stability, Instability and Chaos*, Berlin: Springer, 2008, ch. 7.
- [4] V. Knyva, M. Knyva, J. Rainys, "New approach to calibration of vertical fuel tanks", *Elektronika ir Elektrotechnika*, vol. 19, no. 8, pp. 37–40, 2013.
- [5] Z. S. Velickovic, V. D. Pavlovic, "The performance of the modified gcc technique for differential time delay estimation in the cooperative sensor network", *Elektronika ir Elektrotechnika*, vol. 19, no. 8, pp. 119–122, 2013.
- [6] Tao Deng, Guang-Qiong Xia, Liang-Ping Cao, Jian-Guo Chen, Xiao-Dong Lin, Zheng-Mao Wu, "Bidirectional chaos synchronization and communication in semiconductor lasers with optoelectronic feedback", *Opt. Commun.*, vol. 282, no. 11, pp. 2243–2249, 2009. [Online]. Available: <http://dx.doi.org/10.1016/j.optcom.2009.02.040>
- [7] R. M. Nguimdo, "Optical communications using chaotic carriers generated by electro-optical feedback devices", Ph. D. dissertation, IFIS, Italy, 2008.
- [8] E. V. Grigorieva, H. Haken, S. A. Kaschenko, "Theory of quasiperiodicity in model of lasers with delayed optoelectronic feedback", *Opt. Commun.*, vol. 165, no. 4–6, pp. 279–292, 1999. [Online]. Available: [http://dx.doi.org/10.1016/S0030-4018\(99\)00236-9](http://dx.doi.org/10.1016/S0030-4018(99)00236-9)
- [9] T. Wagenknecht, W. Michiels, K. Green, "Structured pseudospectra for nonlinear eigenvalue problems", *J. Comput. Appl. Math.*, vol. 212, no. 2, pp. 245–259, 2008. [Online]. Available: <http://dx.doi.org/10.1016/j.cam.2006.12.007>
- [10] S. Tang, J. M. Liu, "Chaotic pulsing and quasi-periodic route to chaos in a semiconductor laser with delayed opto-electronic feedback", *IEEE J. Quant. Electron.*, vol. 37, no. 3, pp. 329–336, 2001. [Online]. Available: <http://dx.doi.org/10.1109/3.910441>
- [11] W. K. Hale, S. M. Verduyn Lunel, *Introduction to Functional Differential Equations*, New York: Springer, 1993, ch. 1. [Online]. Available: <http://dx.doi.org/10.1007/978-1-4612-4342-7>
- [12] K. Gu, V. L. Kharitonov, J. Chen, *Stability of Time-Delay Systems*, Basel: Birkhauser, 2003, ch. 1. [Online]. Available: <http://dx.doi.org/10.1007/978-1-4612-0039-0>
- [13] J. J. Loiseau, W. Michiels, S.-I. Niculescu, R. Sipahi, *Topics in Time Delay Systems: Analysis, Algorithms and Control*, Berlin: Springer, 2009, ch. 1. [Online]. Available: <http://dx.doi.org/10.1007/978-3-642-02897-7>
- [14] Zhen Wu, Wim Michiels, "Reliably computing all characteristic roots of delay differential equations in a given right half plane using a spectral method", *J. Comput. Appl. Math.*, vol. 236, no. 9, pp. 2499–2514, 2012. [Online]. Available: <http://dx.doi.org/10.1016/j.cam.2011.12.009>
- [15] K. Engelborghs, T. Luzyanina, D. Roose, "Numerical bifurcation analysis of delay differential equations using DDE-BIFTOOL", *ACM Trans. Mathematical Software*, vol. 28, no. 1, pp. 1–21, 2002. [Online]. Available: <http://dx.doi.org/10.1145/513001.513002>
- [16] T. Vyhlidal, P. Zitek, "Mapping based algorithm for large-scale computation of quasi-polynomial zeros", *IEEE Trans. Autom. Control*, vol. 54, no. 1, pp. 171–177, 2009. [Online]. Available: <http://dx.doi.org/10.1109/TAC.2008.2008345>
- [17] D. Breda, S. Maset, R. Vermiglio, "Computing the characteristic roots for delay differential equations", *IMA J. Numer. Anal.*, vol. 24, no. 1, pp. 1–19, 2004. [Online]. Available: <http://dx.doi.org/10.1093/imanum/24.1.1>
- [18] K. Verheyden, T. Luzyanina, D. Roose, "Efficient computation of characteristic roots of delay differential equations using LMS methods", *J. Comput. Appl. Math.*, vol. 214, no. 1, pp. 209–226, 2008. [Online]. Available: <http://dx.doi.org/10.1016/j.cam.2007.02.025>